Electrophoresis of DNA Adsorbed to a Cationic Supported Bilayer

David J. Olson,† Joseph M. Johnson,‡ Prateek D. Patel,† Eric S. G. Shaqfeh,† Steven G. Boxer,‡ and Gerald G. Fuller*,†

Department of Chemical Engineering and Department of Chemistry, Stanford University, Stanford, California 94305

Received March 28, 2001. In Final Form: July 30, 2001

We report fluorescence microscopy studies of the electrophoresis of individual DNA molecules electrostatically adsorbed to a cationic supported lipid bilayer. Obstacles to uniform electrophoretic flow cause the 2-D chains to adopt hooked conformations similar to those previously observed in 3-D electrophoresis experiments. Analysis of the stretch−contraction dynamics allows for an estimate of the obstacle density in the bilayer. Increasing the electric field causes the DNA molecules to become more highly stretched and increases the electrophoretic mobility substantially. A comparison of the Rouse relaxation time of the polymers and the average time between chain-obstacle collisions reveals that a single-obstacle model is insufficient to describe the observed dynamics but the obstacles are not dense enough to use a reptative model. Analysis of the unhooking dynamics reveals an 80% increase in hydrodynamic drag as compared to free chains. Finally, we observe anomalous diffusion of the DNA chains, with a large increase in the diffusion coefficient after the repeated application of high electric fields. Implications of the flow obstacles in the engineering of separation applications are discussed.

I. Introduction

The direct visualization of individual DNA molecules represents an important advance in studies of polymer dynamics and rheology.[1−3] This body of research includes the examination of the dynamics of DNA in extensional[4,5] and shear[6,7] flows and the mapping of the force−extension curves[8−11] of DNA molecules in three dimensions. In addition, observations of individual DNA chains negotiating obstacle courses (e.g., polymer gels,[12,13] solutions,[14] microfabricated arrays,[15−17] or self-assembled structures[18]) have yielded insight on the physics governing molecular weight separations of polyelectrolytes.[19,20] Maier and Rädler,[21,22] in their recent work on DNA electrostatically adsorbed to a fluid cationic lipid bilayer, found that the chains freely diffused in two dimensions. Exploiting the DNA−lipid bilayer system developed by Maier and Rädler, we study the nonequilibrium dynamics of 2-D polymers by applying an electric field parallel to the bilayer and observing individual, fluorescently labeled, double-stranded DNA molecules as they move electrophoretically. Just as the visualization of individual molecules in response to 3-D flows has provided deep insight into rheological behavior (such as the overshoot in viscosity in transient shear flows[23]), our work visualizing 2-D polymers will aid in the formulation of constitutive equations for complex fluid interfaces.[24−26]

It is important to note that for this system we know a priori of two major sources of variability in the measured properties of the chains. First, single molecule flow experiments have shown that polymer chains exhibit individualism previously undetectable in bulk measurements.[27] Second, there is variability in the preparation of the bilayer itself, evident from the spread of lipid diffusion coefficients measured on different samples (data not shown). We report here results from many different DNA molecules on one bilayer-DNA sample; qualitatively

† Department of Chemical Engineering.
‡ Department of Chemistry.

(1) Ferry, J. D. *Viscoelastic Properties of Polymers*; Wiley: New York, 1980.
(2) Bird, R. B.; Armstrong, R. C.; Hassager, O. *Dynamics of Polymeric Liquids*; Wiley: New York, 1987.
(3) Larson, R. G. *The Structure and Rheology of Complex Fluids*; Oxford University Press: New York, 1999.
(4) Perkins, T. T.; Smith, D. E.; Chu, S. *Science* **1997**, *276*, 2016−2021.
(5) Smith, D. E.; Chu, S. *Science* **1998**, *281*, 1335−1340.
(6) Smith, D. E.; Babcock, H. P.; Chu, S. *Science* **1999**, *283*, 1724−1727.
(7) Doyle, P. S.; Ladoux, B.; Viovy, J. L. *Phys. Rev. Lett.* **2000**, *84*, 4769−4772.
(8) Smith, S. B.; Finzi, L.; Bustamante, C. *Science* **1992**, *258*, 1122−1126.
(9) Perkins, T. T.; Smith, D. E.; Larson, R. G.; Chu, S. *Science* **1995**, *268*, 83−87.
(10) Smith, S. B.; Cui, Y. J.; Bustamante, C. *Science* **1996**, *271*, 795−799.
(11) Meiners, J. C.; Quake, S. R. *Phys. Rev. Lett.* **2000**, *84*, 5014−5017.
(12) Gurrieri, S.; Rizzarelli, E.; Beach, D.; Bustamante, C. *Biochemistry* **1990**, *29*, 3396−3401.
(13) Oana, H.; Masubuchi, Y.; Matsumoto, M.; Doi, M.; Matsuzawa, Y.; Yoshikawa, K. *Macromolecules* **1994**, *27*, 6061−6067.
(14) Schwinefus, J. J.; Morris, M. D. *Macromolecules* **1999**, *32*, 3678−3684.
(15) Volkmuth, W. D.; Duke, T.; Wu, M. C.; Austin, R. H.; Szabo, A. *Phys. Rev. Lett.* **1994**, *72*, 2117−2120.
(16) Duke, T. A. J.; Austin, R. H. *Phys. Rev. Lett.* **1998**, *80*, 1552−1555.
(17) Bakajin, O. B.; Duke, T. A. J.; Chou, C. F.; Chan, S. S.; Austin, R. H.; Cox, E. C. *Phys. Rev. Lett.* **1998**, *80*, 2737−2740.
(18) Doyle, P. S.; Bibette, J.; Deminiere, B.; Viovy, J. L. Magneto-sensitive Self-Organizing Arrays for DNA Separations. *Proceedings of the Society of Rheology 72nd Annual Meeting*, Hilton Head Island, SC, 2001.
(19) Slater, G. W.; Kist, T. B. L.; Ren, H. J.; Drouin, G. *Electrophoresis* **1998**, *19*, 1525−1541.
(20) Viovy, J. L. *Rev. Mod. Phys.* **2000**, *72*, 813−872.
(21) Maier, B.; Radler, J. O. *Phys. Rev. Lett.* **1999**, *82*, 1911−1914.
(22) Maier, B.; Radler, J. O. *Macromolecules* **2000**, *33*, 7185−7194.
(23) Babcock, H. P.; Smith, D. E.; Hur, J. S.; Shaqfeh, E. S. G.; Chu, S. *Phys. Rev. Lett.* **2000**, *85*, 2018−2021.
(24) Edwards, D. A.; Brenner, H.; Wasan, D. T. *Interfacial Transport Processes and Rheology*; Butterworth-Heinemann: Boston, 1991.
(25) Fuller, G. G. *Curr. Opin. Colloid Interface Sci.* **1997**, *2*, 153−157.
(26) Olson, D. J.; Fuller, G. G. *J. Non-Newtonian Fluid Mech.* **2000**, *89*, 187−207.
(27) de Gennes, P. G. *Science* **1997**, *276*, 1999−1999.

10.1021/la010475j CCC: $20.00
Published on Web 10/12/2001

similar conformations and dynamics were observed for all samples tested.

II. Materials and Methods

1,2-Dioleoyl-3-trimethylammonium-propane (DOTAP, cationic) and 1,2-dioleoyl-*sn*-glycero-3-phosphocholine (DOPC, neutral) were used as purchased from Avanti Polar Lipids (Alabaster, AL). Cationic lipid vesicles were prepared by first mixing the lipids in a 10 mol % DOTAP:90 mol % DOPC ratio in chloroform. After the solvent evaporated, the lipids were resuspended in Millipore water at a concentration of 5 mg/mL and extruded unilamellar vesicles (EUVs)[28,29] were formed. The supported lipid bilayer was assembled by vesicle fusion[30] of EUVs to a glass coverslip. Prior to vesicle fusion, coverslips were boiled for 1 h in 7X detergent (ICN Biochemicals, Aurora, OH), rinsed thoroughly with distilled water, dried under a nitrogen stream, and heated to 400 °C for 4 h. A sample cell was prepared with two clean coverslips separated by 75 μm Kapton tape and sealed with a small amount of epoxy on two parallel edges. The EUV dispersion was flowed into the coverslip sandwich by capillary motion and incubated for 10 h, forming a fluid lipid bilayer. The sample cell was subsequently rinsed with 10 mM HEPES (*N*-(2-hydroxyethyl)piperazine-*N*′-ethanesulfonic acid) buffer to remove unfused vesicles.

λ-DNA (48,502 bp; Gibco BRL, Gaithersburg, MD) was cleaved with the restriction enzyme *Sfo1* (New England Biolabs, Beverly, MA) and then fluorescently stained with YOYO-1 (Molecular Probes, Eugene, OR) at a nominal 5:1 base pair to dye molecule ratio. *Sfo1* cleaves the DNA at the 45 679th base pair, leaving a blunt end to ensure that the DNA molecule was not circularized. A dilute aqueous solution of the cleaved DNA was sequentially dialyzed against 10 mM HEPES/100 mM EDTA (ethylenediaminetetraacetic acid) and 10 mM HEPES/1 mM EDTA to remove divalent cations, which promote condensation of DNA. All buffers used in the preparation and experiments were titrated to pH 7. The two fluorescently labeled restriction fragments have contour lengths of approximately 20 and 1 μm.[9]

DNA molecules were electrostatically adsorbed to the cationic bilayer by first incubating them with the bilayer for 10 min and then rinsing with 10 mM HEPES/10 mM NaCl/0.1 wt % ascorbic acid. The concentration of DNA in this buffer was chosen such that the final surface density of molecules was sufficiently low so that inter-DNA interactions could be neglected. Ascorbic acid was added to scavenge molecular oxygen, which would otherwise increase the photosensitization of the DNA−dye complex.[31] Ascorbic acid was chosen because fluorescence images revealed that other common oxygen scavengers, such as β-mercaptoethanol and glucose oxidase, had deleterious effects on the bilayer. The ascorbic acid buffer was bubbled with argon for at least 30 min before experiments to further reduce the amount of dissolved oxygen.

A delrin sample holder was designed such that the open edges of the coverslip sandwich were in contact with two buffer reservoirs, each of which contained an electrode allowing for the application of an electric field parallel to the bilayer.[32] Molecules were visualized on a Nikon Eclipse TE300 inverted microscope equipped with a 100× oil-immersion (NA = 1.4) objective. A PentaMAX Gen IV intensified CCD camera (Princeton Instruments, Trenton, NJ) was used to capture and transfer the images to a PC. The particle tracking algorithm included in MetaMorph software (Universal Imaging Corp., West Chester, PA) was used to track the centers of mass of DNA molecules for diffusion coefficient and mobility calculations. Chain extensions, L_x, were quantified by measuring the projection of the polymer conformation onto the vector defining the electric field. This length is, in general, different than the end-to-end length typically used in polymer scalings, but recent simulations have shown that these two quantities can be used interchangeably to describe polymer dynamics.[33] As defined, the average extension of chains at equilibrium is twice the radius of gyration, R_g.

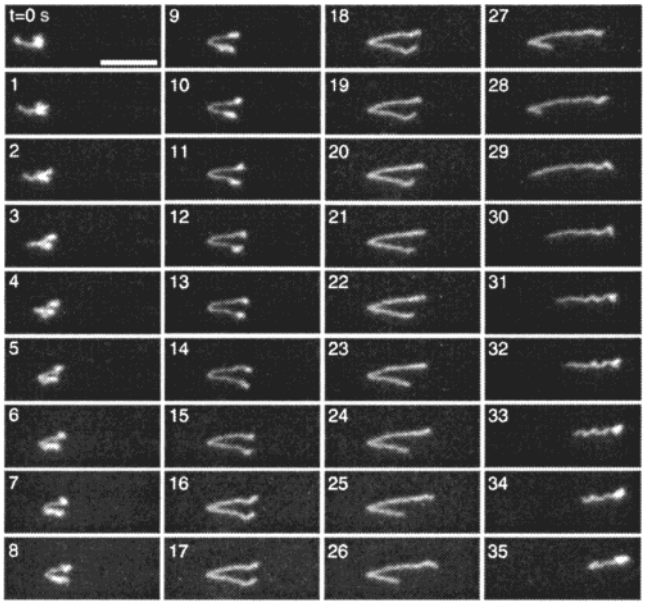

Figure 1. DNA molecule encountering an obstacle in the bilayer. The electric field (E = 3.3 V/cm) points to the left. Elapsed time (in seconds) is indicated in each panel. Scale bar = 10 μm.

III. Results and Discussion

Maier and Rädler have observed that hydrodynamic interactions in DNA adsorbed to a cationic bilayer are screened due to the proximity to the solid substrate.[21,22] One would expect that these molecules would translate in an unstretched conformation in response to an electric field because the electrophoretic and hydrodynamic forces are equally distributed between all polymer segments. However, in our experiments, the DNA molecules were unexpectedly observed to encounter obstacles to uniform electrophoretic flow, causing them to stretch. A time lapse illustrating the interaction between a typical chain and an obstacle is shown in Figure 1. As the molecule encounters the obstacle, it initially adopts a U-shaped conformation (t = 0−19 s), corresponding to the middle portion of the molecule hooked on the obstacle with the two free ends of the molecule extended in the direction of flow. Once fully stretched, the longer of the two arms, which experiences a net electrophoretic force, pulls the rest of the molecule around the obstacle, similar to a rope moving around a pulley (t = 20−28 s). The chain reaches its maximum extension precisely when the trailing end is freed from the obstacle (t = 29 s), after which the molecule snaps quickly back toward a coil-like conformation due to the entropic elasticity of the chain.

The stretch−contraction dynamics of chains migrating along the bilayer can be used to estimate the obstacle density, assuming that each spike in the extension of the chain corresponds to a chain-obstacle collision. Figure 2a plots the time evolution of the extension and instantaneous velocity for a typical molecule. As the molecule encounters obstacles (t = 16, 58, 104, 133, and 157 s), a local maximum in the extension is achieved, followed immediately by a sharp peak in the velocity as the molecule rapidly retracts back toward its equilibrium conformation. Similar con-

(28) Mayer, L. D.; Hope, M. J.; Cullis, P. R. *Biochim. Biophys. Acta* **1986**, *858*, 161−168.
(29) MacDonald, R. C.; MacDonald, R. I.; Menco, B. P. M.; Takeshita, K.; Subbarao, N. K.; Hu, L. R. *Biochim. Biophys. Acta* **1991**, *1061*, 297−303.
(30) Brian, A. A.; McConnell, H. M. *Proc. Natl. Acad. Sci. U.S.A.* **1984**, *81*, 6159−6163.
(31) Akerman, B.; Tuite, E. *Nucleic Acids Res.* **1996**, *24*, 1080−1090.
(32) Groves, J. T.; Boxer, S. G. *Biophys. J.* **1995**, *69*, 1972−1975.
(33) Hur, J. S. Personal communication.

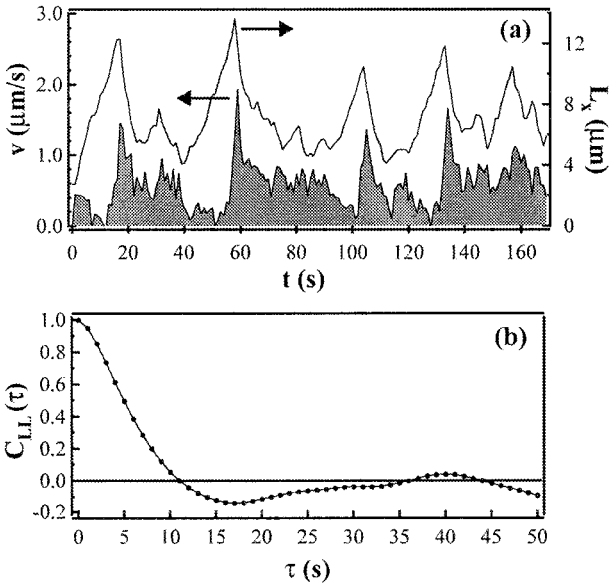

Figure 2. (a) Time evolution of the velocity (shaded curve) and extension (unshaded curve) of a DNA molecule undergoing electrophoretic flow through an array of obstacles. (b) Autocorrelation of extension data, averaged for 10 molecules. The fundamental time scale between collisions is seen to be approximately 40 s. $E = 3.3$ V/cm.

formations and a correspondence between the velocity and the extension have been reported in fluorescence visualization experiments on DNA in gels[13] and dilute polymer solutions.[14]

Figure 2b plots the time autocorrelation of the extension

$$C_{LL}(\tau) = \frac{\sum \delta L_x(t)\delta L_x(t+\tau)}{\sum [\delta L_x(t)]^2} \quad (1)$$

where $\delta L_x(t)$ is the fluctuation of the extension about the average. The fundamental time interval between encounters with obstacles is shown to be approximately 40 s. Multiplying by the average velocity (0.58 μm/s at 3.3 V/cm) gives a rough estimate of 23 μm between chain-obstacle collisions. To estimate the obstacle density, we divide the time interval between chain-obstacle collisions into two regimes: one where the polymer migrates in an extended conformation and one where the chain travels in a coiled conformation. In the stretched regime, the probability of the leading end of the 2-D chain encountering an obstacle is greatly reduced due to the decrease in cross-sectional width. Therefore, we use the coiled regime to estimate the obstacle spacing. During collisions, the chains reach an extension of roughly 10−14 μm at $E = 3.3$ V/cm (see Figure 2a). Once the trailing end is freed from the obstacle, the molecule relaxes back to a coil-like conformation on a time scale of about 5 s (see Figure 1), during which the molecule translates a distance of approximately 13−17 μm (the sum of the obstacle-induced extension and the average electrophoretically driven migration during the relaxation time scale). Therefore, the average chain travels about 6−10 μm in a coiled conformation before impinging on another obstacle. Using the average cross-sectional width of approximately 3 μm for a chain in its coiled conformation (determined from our fluorescence images), we estimate the obstacle density as $\rho_{obs} = 0.03-0.05\ \mu m^{-2}$.

This is most likely the lower limit for the obstacle density, as we are neglecting the possibility of collisions between a chain and multiple obstacles. These multiple collision events are evident in Figure 3a, which is a

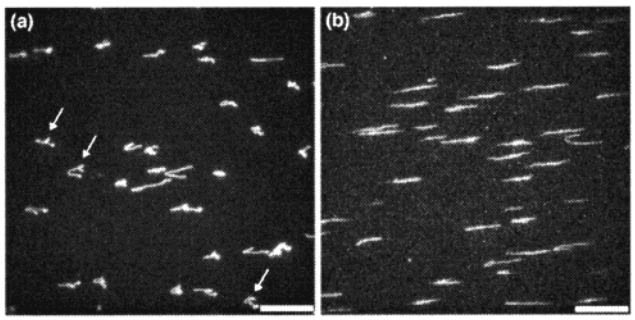

Figure 3. Snapshots of DNA molecules undergoing electrophoresis at (a) $E = 3.3$ and (b) 53.3 V/cm. The chains are weakly stretched at the low electric field and sometimes collide with multiple obstacles (denoted by arrows). At the high field, the chains are much more highly stretched and do not collide with multiple obstacles. Scale bar = 20 μm.

snapshot of the electrophoresis of DNA molecules at $E =$ 3.3 V/cm. Note, however, that as the electric field is increased to 53.3 V/cm (Figure 3b), no multiple collisions are observed. Additionally, in the extension autocorrelation analysis, we are only considering events in which the chain is significantly extended by the encounter with an obstacle. Saville and Sevick describe an alternative "roll-off" mechanism of chain release from an obstacle that does not induce strong stretching in the chain.[34] This interaction mechanism is most likely not the dominant one, since the conformations in Figure 1 strongly suggest that the obstacle size is much smaller than the radius of gyration of the chains.

As the electric field is increased, chains that are hooked on obstacles become more highly stretched. The degree of stretching can be described by the Péclet number, a dimensionless measure of the electrophoretic force:

$$Pe = E\lambda a/kT \quad (2)$$

Here, E is the electric field, a is the Kuhn step (132 nm for fluorescently labeled DNA[6]), λ is the charge per Kuhn step, and kT is the thermal energy. The Péclet number corresponds to the ratio of the diffusive time scale ($\tau_{diff,KS} = a^2\zeta/kT$) to the electrophoretic convective time scale ($\tau_{conv,KS} = \zeta a/E\lambda$), where ζ is the hydrodynamic drag coefficient. For $Pe > 1$, the electrophoretic energy dominates the thermal energy and a tethered chain becomes stretched. Conversely, for $Pe < 1$, Brownian motion is sufficient to resist electrophoretic stretching.

To calculate the charge per Kuhn step, one must consider the electrostatic interaction of a polyelectrolyte and an oppositely charged surface.[35−38] Sens and Joanny determined that the adsorption of a polyelectrolyte to a surface whose charges are mobile (such as a lipid bilayer) is accompanied by a total release of the condensed counterions (present in free solution due to the high linear charge density of DNA).[38] Once the DNA is adsorbed, the mobile cationic lipids behave as 2-D confined counterions[35] and will undergo Manning condensation.[39,40] Manning condensation leads to a renormalized linear charge density of e/l_B, where $l_B = e^2/4\pi\epsilon\epsilon_0 kT$ is the Bjerrum length. Here, e is the charge of an electron, ϵ is the dielectric constant of the solution, and ϵ_0 is the permittivity of free space. In

(34) Saville, P. M.; Sevick, E. M. *Macromolecules* **1999**, *32*, 892−899.
(35) Bruinsma, R.; Mashl, J. *Europhys. Lett.* **1998**, *41*, 165−170.
(36) Menes, R.; Pincus, P.; Pittman, R.; Dan, N. *Europhys. Lett.* **1998**, *44*, 393−398.
(37) Netz, R. R.; Joanny, J. F. *Macromolecules* **1999**, *32*, 9013−9025.
(38) Sens, P.; Joanny, J. F. *Phys. Rev. Lett.* **2000**, *84*, 4862−4865.
(39) Manning, G. S. *J. Chem. Phys.* **1968**, *51*, 924.
(40) Oosawa, F. *Biopolymers* **1968**, *6*, 1633.

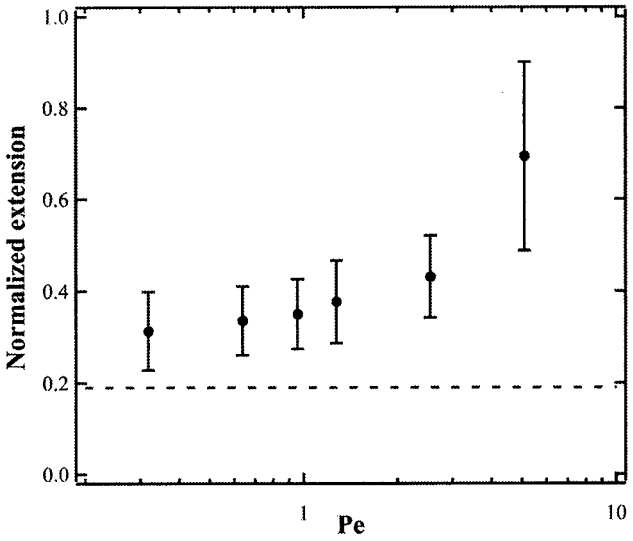

Figure 4. Average extension of chains (normalized by the contour length) as a function of *Pe*. Error bars correspond to standard deviations determined from a Gaussian fit to histograms of extension (1000 molecules). Dashed line denotes equilibrium extension ($2R_g/Na$). The extension monotonically increases with *Pe*, with a rather abrupt increase between $Pe = 3$ and 5. Note that even at low *Pe*, the molecules remain stretched beyond the equilibrium conformation.

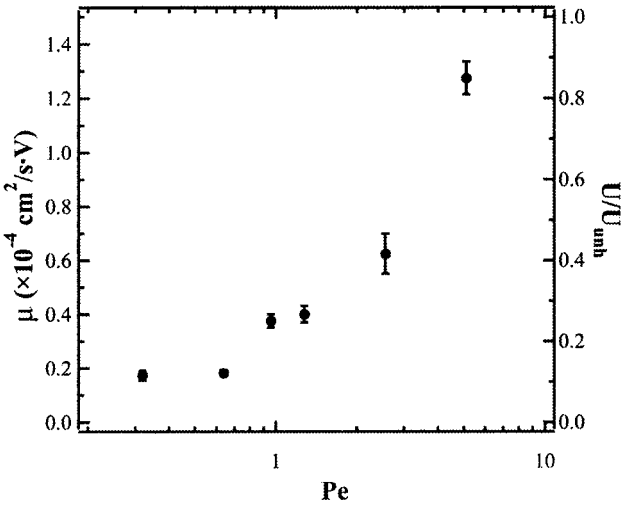

Figure 5. Electrophoretic mobility and dimensionless velocity of DNA chains as a function of *Pe*. The average velocity is nondimensionalized by the unhindered velocity, U_{unh}, measured experimentally at $Pe = 5.1$ and linearly scaled for lower *Pe* (see text). The mobility is constant for low *Pe* but exhibits a strong dependence on *Pe* for $Pe > 0.64$. The dimensionless velocity, which reports the "effectiveness" of the obstacles in impeding the chains, decreases strongly as *Pe* decreases.

water at room temperature, $l_B = 7$ Å, giving an effective linear charge density of $\lambda = 2.97 \times 10^{-17}$ C/Kuhn step. When this charge density and the Kuhn step length for fluorescently labeled DNA is used, $Pe = 0.096E$, where E is expressed in V/cm.

Figure 4 illustrates as a function of *Pe* the average chain extension, nondimensionalized by the contour length of the DNA (20 μm). Over 1000 conformations were ensemble averaged for each *Pe*, and the error bars correspond to the standard deviation calculated from Gaussian fits to chain extension histograms. The average extension is observed to monotonically increase as a function of *Pe*, with an abrupt increase in extension between $Pe = 2.5$ and 5.1. For $Pe < 5.1$, the chains are rarely stretched more than 50% of the contour length, while at $Pe = 5.1$ the chains exist almost exclusively in highly stretched conformations (>50%).

As mentioned previously, chains with high degrees of extension have a reduced probability of becoming ensnared on obstacles. Recent simulations of field-driven polymers colliding with fixed obstacles have shown that the center-of-mass velocity of chains hooked around obstacles is decreased relative to nonimpacting chains.[41] In Figure 5, we plot the electrophoretic mobility, $\mu = v/E$, of the chains as a function of *Pe*. At low *Pe* ($Pe < 0.64$), the mobility appears constant, while at higher *Pe* the mobility is a strongly increasing function of *Pe*.

This transition between a constant mobility and an increasing mobility as the electric field is increased bears striking resemblance to the data reported by Heller et al. from their studies of DNA electrophoresis in agarose gel.[42] Their data are consistent with a transition from unoriented reptation to oriented reptation in the framework of the biased reptation with fluctuations model.[43] In the agarose gel system, the pore size, $b \approx 250-500$ nm, yields a ratio of the Kuhn step (100 nm) to the pore size, $a/b = 0.2-0.4$. However, for our system, we can estimate the pore size as $b = \rho_{obs}^{-1/2} = 4.5-5.8$ μm, giving $a/b = 0.023-0.03$. For this estimate of the obstacle density, reptation is not likely to be an accurate description of the polymer migration. In fact, for the ratio of Kuhn step to pore size to approach that of typical gel electrophoresis, the actual obstacle density would have to be 2 orders of magnitude greater than the current estimate.

Figure 5 also plots the DNA migration data in terms of a velocity nondimensionalized by an unhindered velocity, U_{unh}. U_{unh} was experimentally measured at the highest *Pe* by visually selecting molecules that were not interacting with obstacles and manually determining their velocities. A local force balance on the chain yields the following formula

$$U_{unh} = E\lambda N/\zeta \tag{3}$$

which was used to calculate U_{unh} for lower *Pe*. Here, $N = 150$ is the number of Kuhn steps, and ζ is the hydrodynamic drag coefficient, which was assumed to remain constant for all *Pe*. At $Pe = 5.1$, $U_{unh} = 80$ μm/s, giving $\zeta = 2.97 \times 10^{-7}$ Ns/m. At $Pe = 5.1$, the obstacles reduce the velocity of the chains to 85% of the unhindered velocity, while at lower *Pe* the obstacles are significantly more effective at impeding the velocity of the chains ($U/U_{unh} \approx 0.12$ for $Pe = 0.32$ and 0.64).

In their treatment of an individual, field-driven polymer interacting with a single post, Sevick and Williams calculated the velocity of a polymer traveling through a dilute array of posts relative to the velocity of a free chain[41]

$$\langle U \rangle / U_{unh} = 1 - B\rho_{obs}N^{3/2} \tag{4}$$

where B is a numerical constant. In their work, they considered only the high electric field regime, $Pe \gg 1$. For this model to apply to our experimental system, the obstacles need to be dilute enough so that the polymer has time to relax from its stretched conformation before encountering another obstacle; that is, the ratio of the polymer relaxation time to the average time between

(41) Sevick, E. M.; Williams, D. R. M. *Phys. Rev. Lett.* **1996**, *76*, 2595−2598.
(42) Heller, C.; Duke, T.; Viovy, J. L. *Biopolymers* **1994**, *34*, 249−259.
(43) Semenov, A. N.; Duke, T. A. J.; Viovy, J. L. *Phys. Rev. E: Stat. Phys., Plasmas, Fluids, Relat. Interdiscip. Top.* **1995**, *51*, 1520−1537.

collisions must be small. The longest relaxation time for a 2-D bead-rod chain is given by

$$\tau_{\text{relax}} \approx 0.021(\zeta a^2/NkT)N^2 \tag{5}$$

The drag coefficient calculated from the unhindered velocity yields a relaxation time of 6.2 s, which is consistent with the relaxation observed in Figure 1 but an order of magnitude greater than λ-DNA in water.[4] It has been shown recently that the confinement of DNA chains to increasingly thin gaps (from 5 to 0.09 μm) increases the relaxation time by a factor of approximately 3,[17] and one would expect that as the polymer is strictly confined to two dimensions,[37] this effect would be enhanced. The average time between collisions is equal to the reciprocal of the collision frequency, which can be determined by multiplying the area traversed per unit time ($\sim 2U_{\text{unh}}R_g$) by the obstacle density:

$$\tau_{\text{collision}} = \frac{1}{2U_{\text{unh}}R_g\rho_{\text{obs}}} = \frac{6^{1/2}\zeta b^2}{2E\lambda a N^{3/2}} \tag{6}$$

The ratio of the two time scales is

$$\beta = \frac{\tau_{\text{relax}}}{\tau_{\text{collision}}} \approx 0.025\frac{a^2}{b^2}N^{5/2}Pe \tag{7}$$

For our system ($a = 0.132$ μm, $b \approx 5$ μm, and $N = 150$), $\beta = 4.9Pe$. Additionally, if our obstacle density is a low estimate, as supposed previously, β would increase even further. Obviously, the condition $\beta \ll 1$ cannot be satisfied at any reasonable electric field strength, and therefore, the polymers do not have sufficient time to relax fully between collisions. This is evident in Figure 4, where, even at $Pe = 0.32$ ($\beta = 1.57$), the normalized extension rarely approaches the equilibrium value ($2R_g/Na$). However, the overall stretch is not extremely large because Pe is still small.

It appears that our polymer−obstacle system is in a state intermediate to that of a single-post collision regime and a reptative regime. Numerical simulations are perhaps the best way to determine the physical phenomena causing the strong dependence of electrophoretic mobility on Pe. To understand more clearly the interaction between the polymer chains and the obstacles, we studied the unhooking dynamics of the molecules in detail, following the model of Volkmuth et al.[15] A chain asymmetrically hooked on an obstacle feels a net electrophoretic force proportional to the difference in the arm lengths, which we define as x. By balancing the electrophoretic force with the hydrodynamic drag along the contour of the molecule, one can derive the following equation for the time evolution of x:

$$(1/2)\zeta(\mathrm{d}x/\mathrm{d}t) = E\lambda x/a \tag{8}$$

Note that the equation derived in Volkmuth et al.[15] is missing the factor of $^1/_2$ relating the velocity along the chain contour to dx/dt. Solving eq 8 yields an exponential time dependence of $x(t) = x_0 \exp(t/\tau)$, with a time constant

$$\tau = \frac{a\zeta}{2E\lambda} = \frac{N}{2}\frac{\tau_{\text{diff,KS}}}{Pe} \tag{9}$$

Therefore, the time constant is simply equal to the time it takes for a segment of the polymer to electrophoretically migrate a distance of $N/2$ Kuhn steps. For the two lowest Pe, we have examined the unhooking dynamics of chains manually determined not to undergo multiple collisions with obstacles (at higher Pe, the chain velocities are too fast to gather a sufficient number of data points with which to fit an exponential curve). Figure 6 plots the time evolution of $x(t)/x_0$ averaged over 10 molecules at $Pe = 0.32$ and 0.64. In the semilog plot, the data are fit extremely well by a line whose slope, $1/\tau$, is indeed proportional to Pe. Using eq 9, we can calculate a drag coefficient from the slope, $\zeta = 2E\lambda\tau/a = 5.38 \times 10^{-7}$ Ns/m. As compared to the drag coefficient calculated from the unhindered velocity ($\zeta = 2.97 \times 10^{-7}$ Ns/m), the obstacle−chain interaction increases the effective hydrodynamic drag by 80%.

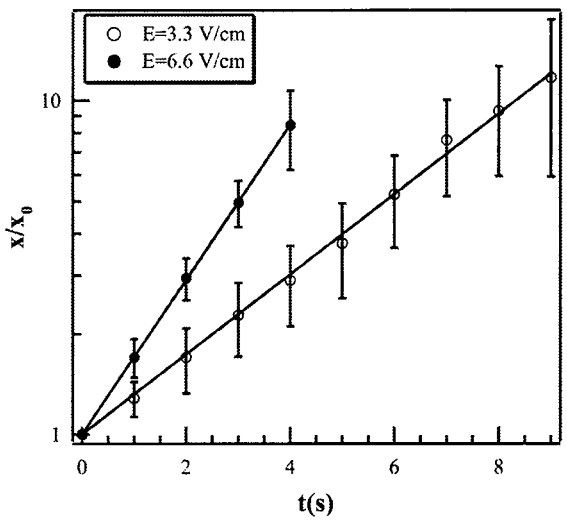

Figure 6. Time evolution of arm length difference as determined from analysis of unhooking dynamics of chains from obstacles, averaged over approximately 20 molecules for each Pe. The data are fit by exponential functions, $x/x_0 = \exp(t/\tau)$, with $\tau = 3.62$ s for $Pe = 0.32$ and $\tau = 1.87$ s for $Pe = 0.64$.

Finally, the presence of obstacles appears to affect the equilibrium dynamics of the polymers. For a freely diffusing object in a purely viscous solvent, the mean-squared displacement of chains (MSD), $\langle x^2(t)\rangle$, will exhibit a linear dependence on time. However, as shown in Figure 7, we observe anomalous diffusion (characterized by a MSD that scales as t^α, with $\alpha < 1$) of the DNA molecules for all times. These data represent ensemble averages (over approximately 30 molecules) of the MSD of chains observed both before the electrophoresis experiments were performed and after the electrophoresis experiments were performed. The data taken before and after the series of electrophoresis experiments are both subdiffusive, with the data after the electrophoresis experiments scaling as $t^{0.55}$. Subdiffusive behavior has been reported in the simulations of Saxton of a diffusing body in a random array of obstacles[44,45] and was also noted by Maier and Rädler for a small population of chains.[22] Anomalous diffusion is often reported in terms of a time-dependent diffusion coefficient,[44] such that $\langle x^2(t)\rangle = 4D(t)t$. The decreasing $D(t)$ observed for both data sets (see Figure 7 inset) suggests that the DNA is somehow confined over these time scales. For purposes of comparison, $D(t)$ at $t = 100$ s is 6.15×10^{-4} μm^2/s before electrophoresis and 1.20×10^{-2} μm^2/s after electrophoresis. It is unknown what mechanism allows the DNA to diffuse more freely after application of an electric field; however, it may be due to effects of the electric field on the cationic lipids and the soluble counterions solvating the DNA chains. No

(44) Saxton, M. J. *Biophys. J.* **1994**, *66*, 394−401.
(45) Saxton, M. J. *Biophys. J.* **1997**, *72*, 1744−1753.

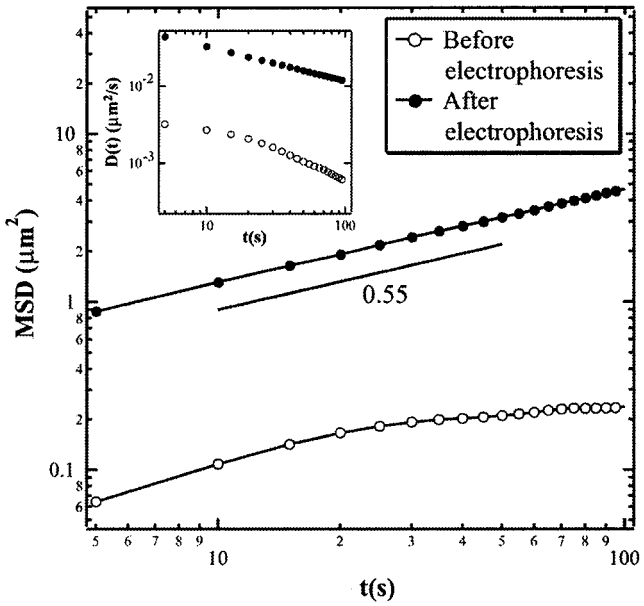

Figure 7. MSD of DNA chains as a function of time (ensemble averaged over approximately 30 chains). Chain diffusion was observed before the series of electrophoresis experiments and after the electrophoresis experiments. Subdiffusive behavior is exhibited in both cases (line of slope = 0.55 is shown to guide the eye). Inset: Time-dependent diffusion coefficient, calculated using $\langle x^2(t)\rangle = 4D(t)t$. The diffusion coefficient of the chains after electrophoresis is roughly 20 times greater than before electrophoresis.

decrease to original diffusive behavior was observed after cessation of electrophoresis for short observation times (~30 min).

IV. Conclusions

We have observed the existence of obstacles in the cationic lipid bilayer that affect both the diffusion and the electrophoresis of DNA chains electrostatically adsorbed to the surface. Whatever the origin of these obstacles,[46] we note that they are not observable by optical microscopy and they have no measurable effect on the electrophoretic motion of dye-labeled lipids or the smaller restriction fragments (≈2800 bp). The similarity between the chain conformations shown in Figure 1 and those observed in bulk electrophoresis[13,14] suggests that these bilayers could be used for molecular weight separations of DNA. Indeed, the smaller restriction fragments were observed to electrophorese more quickly than the large fragments (data not shown). The ability to control the arrangement and density of obstacles (e.g., micropatterning a supported bilayer[47]) would allow for the separation of macromolecules in supported bilayers[48] or in 3-D[49] using defined barriers. Numerical simulations of chains forced electrophoretically through a random array of obstacles at various densities would help elucidate the physical phenomena responsible for the observed dependence of extension and mobility on *Pe*. Finally, this work represents the first direct visualization of the flow properties of polymers strictly confined to two dimensions,[37] which is crucial for the development of constitutive equations for complex interfaces.

Acknowledgment. This work was supported by a Kodak graduate research fellowship (D.J.O.) and CPIMA (Center for Polymeric Interfaces and Macromolecular Assemblies), an NSF-MRSEC sponsored partnership between Stanford University, IBM Almaden Research Center, and the University of California−Davis. The authors also thank B. Maier and J. O. Rädler for offering helpful advice on sample preparation.

LA010475J

(46) Recent experiments in which buffer is flowed between the two coverslips suggest that obstacles are not defects in the bilayer. Subject to hydrodynamic drag, the DNA molecules are again observed to adopt hooked conformations, but the hooking point (obstacle) is now seen to translate in the direction of hydrodynamic flow. In contrast, during electrophoresis experiments, the hooking points remain stationary. It would be expected that bilayer defects would be stationary in hydrodynamic flow and during electrophoresis. If the defects were unfused vesicles, it is possible that they could be translated in hydrodynamic flow. The obstacles could also consist of microdomains of cationic lipids. Electrophoretic forces would act in the opposite direction on cationic domains as they would on DNA chains; however, in hydrodynamic flow, there would be no counterforce acting on the domains. The lack of a counterforce could explain the mobility of cationic domains in hydrodynamic flow as opposed to their immobility during electrophoresis.

(47) Hovis, J. S.; Boxer, S. G. *Langmuir* **2000**, *16*, 894−897.

(48) van Oudenaarden, A.; Boxer, S. G. *Science* **1999**, *285*, 1046−1048.

(49) Chou, C. F.; Bakajin, O.; Turner, S. W. P.; Duke, T. A. J.; Chan, S. S.; Cox, E. C.; Craighead, H. G.; Austin, R. H. *Proc. Natl. Acad. Sci. U.S.A.* **1999**, *96*, 13762−13765.